

# Simulating the two-dimensional electronic spectroscopy of vibronic systems with multiple excited states.

Dale Green\*<sup>1</sup>, Ismael A. Heisler<sup>1</sup> and Garth A. Jones<sup>1</sup>

<sup>1</sup> School of Chemistry, University of East Anglia, Norwich Research Park, Norwich, Norfolk, United Kingdom, NR4 7TJ

e-mail: Dale.Green@uea.ac.uk

## Introduction

In this work, we model the 2D optical spectroscopy of a zinc-porphyrin chromophore with multiple excited states, using two approaches.<sup>1,2</sup> The Multimode Brownian Oscillator (MBO) model calculates the third order molecular response functions using the cumulant expansion.<sup>3,4</sup> Whilst the Equation of Motion-Phase Matching Approach (EOM-PMA) calculates the polarisation in the phase-matched direction from a series of quantum dynamical simulations.<sup>5</sup>

## Linear absorption spectrum of zinc-porphyrin chromophore

Figure 1 identifies three singlet states for the zinc-porphyrin chromophore. The first, the *Q* band, is split into two orthogonal components.

$Q_x$  shows a vibronic absorption at  $15545\text{ cm}^{-1}$ , corresponding to a metal-pyrrole breathing mode of  $380\text{ cm}^{-1}$ , which has been studied using 2D spectroscopy.<sup>1,2</sup>

Whilst the *B* band has little influence on these 2D spectra, as the very broad *N* band is located at twice the frequency of  $Q_x$ , excited state absorption (ESA) pathways become involved.

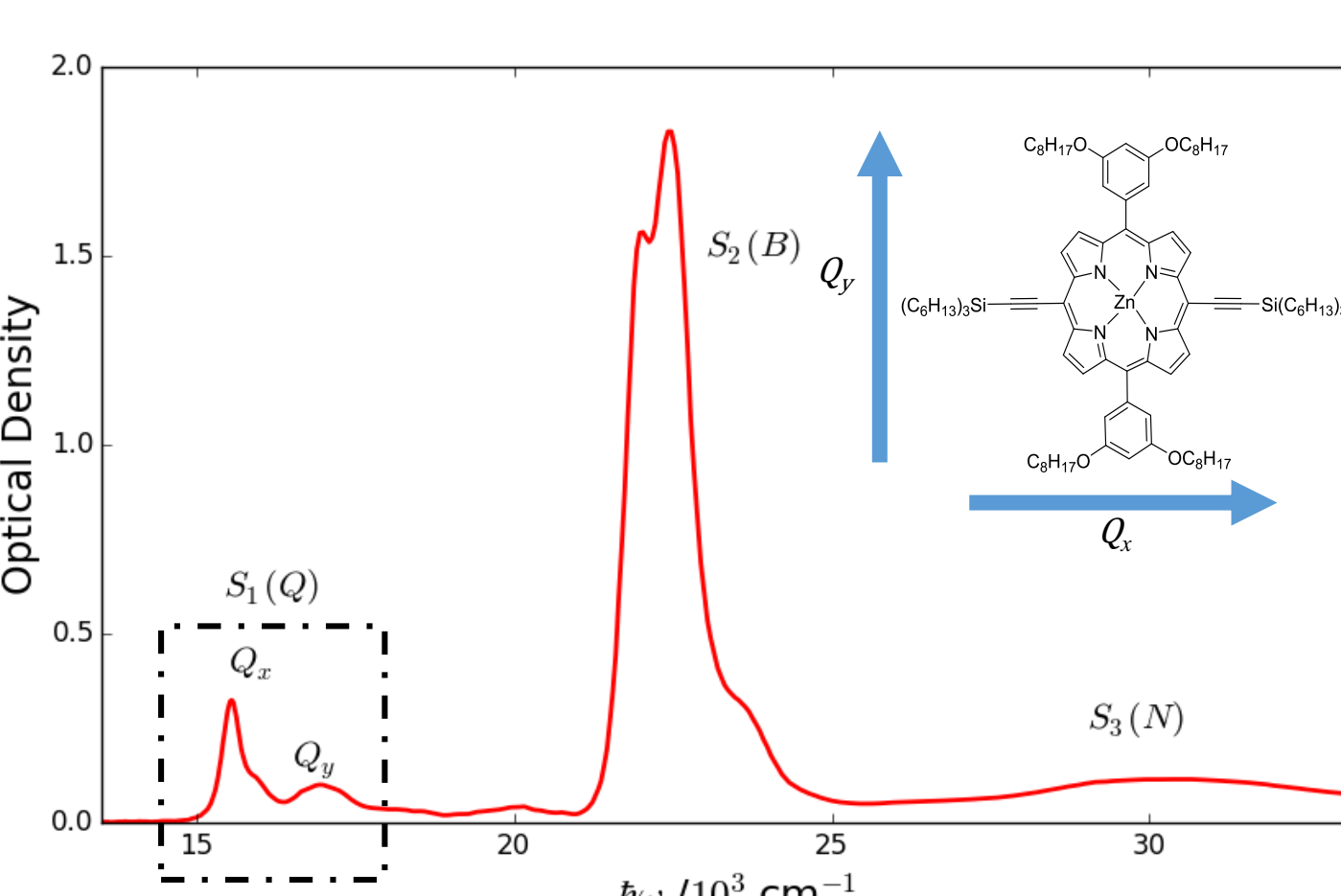


Figure 1: Linear absorption spectrum of the bis-alkynyl zinc-porphyrin chromophore. Inset shows the structure of the chromophore and the directional dipole moments for the *Q* band, which is highlighted.<sup>2</sup>

## 3 level displaced Harmonic oscillator model

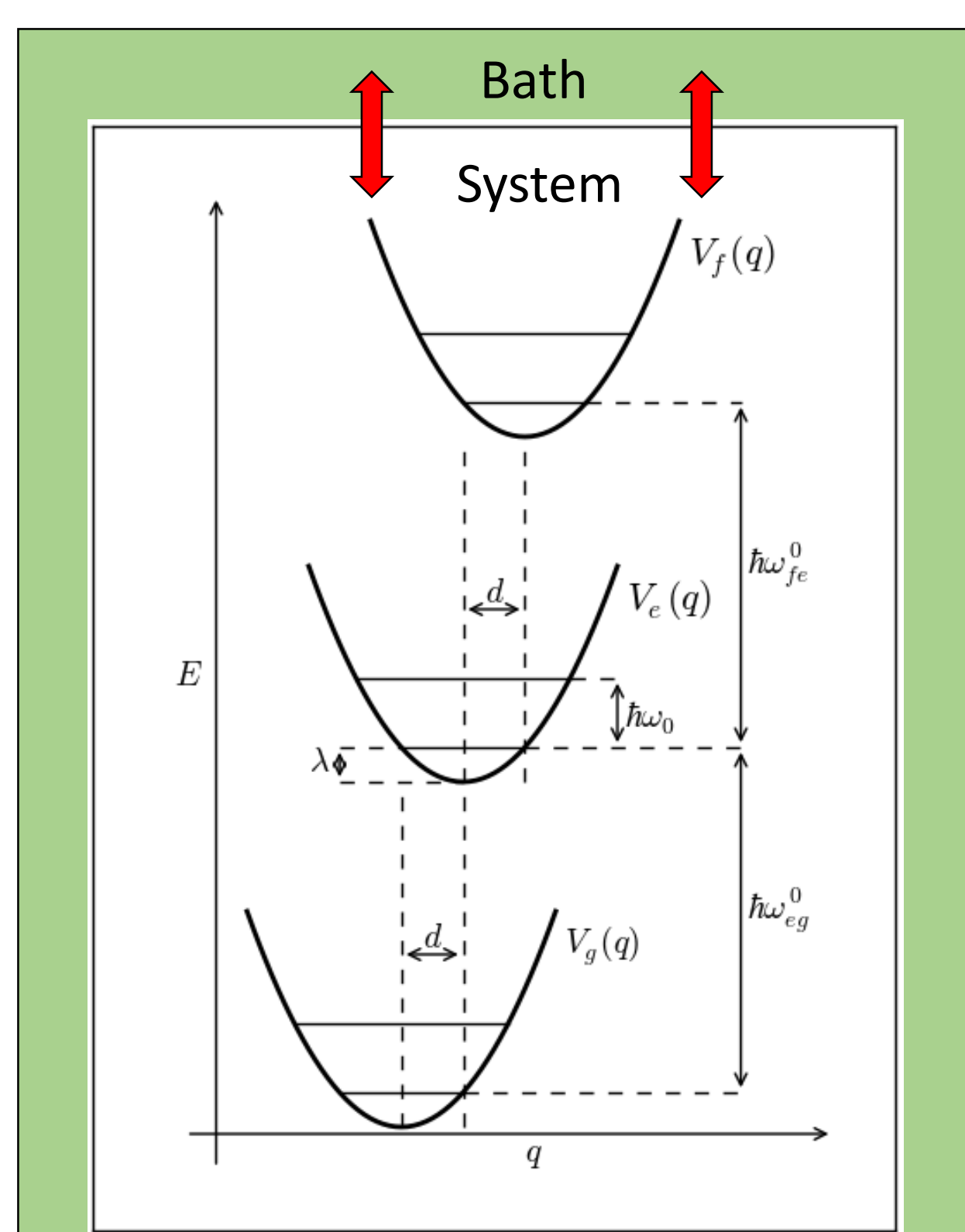


Figure 2: Diagram representing the interaction of the wider bath with the system.

We model the  $S_0$ ,  $S_1$  and  $S_3$  states of the zinc-porphyrin system by coupling three electronic states  $|g\rangle$ ,  $|e\rangle$ , and  $|f\rangle$  to a single harmonic vibrational mode of frequency  $\omega_0$ . Each excited state is displaced along the mode coordinate ( $q$ ) by  $d$  resulting in the reorganisation energy,  $\lambda$ .

$$H_S = |g\rangle h_g \langle g| + |e\rangle (h_e + \hbar\omega_{eg}^0) \langle e| + |f\rangle (h_f + \hbar\omega_{ef}^0) \langle f|$$

$$h_i = \hbar\omega_0 \left( b^\dagger b + \frac{1}{2} - \frac{d}{\sqrt{2}} (b^\dagger + b) \right) \text{ where } i = g, e, f$$

### Assumptions

- We limit each excited state to the first two vibrational levels.
- We assume the two transition frequencies and displacements between states to be equal.

$$\omega_{fe}^0 = \omega_{eg}^0$$

\*This does not account for the full width of the *N* band, but suitably simplifies the quasi-continuum.

## Equation of Motion-Phase Matching Approach

### Theory:

The molecular vibration is included in the system Hamiltonian,  $H_S$ . The laser field is introduced by three Gaussian pulses in the interaction Hamiltonian,  $V_n(t)$ . Separate baths for electronic and vibrational transitions are described by Ohmic spectral densities,  $J(\omega)$ .

$$V_n(t) = \hat{\mu} \cdot (\chi_n E_n(t - \tau_n) e^{(-i\omega_n t + ik_n r)})$$

Seven auxiliary master equations are evolved using Lindblad relaxation dynamics, before being combined to calculate the third order polarisation in the rephasing direction.

$$\dot{\rho}_1(t) = -\frac{i}{\hbar} [H_S - V_1(t) - V_2^\dagger(t) - V_3^\dagger(t), \rho_1(t)] + \sum_{k=e/vib} \gamma_k \left( A_k \rho(t) A_k^\dagger - \frac{1}{2} (A_k^\dagger A_k, \rho_1(t)) \right)$$

$$P_{k_s}^{(3)}(\tau, T, t) = e^{k_s r} \langle \hat{\mu} (\rho_1(t) - \rho_2(t) - \rho_3(t) + \rho_4(t) - \rho_5(t) + \rho_6(t) + \rho_7(t)) \rangle$$

### Parameters (at 300 K)

$$\omega_{eg}^0 = \omega_{fe}^0 = 15545\text{ cm}^{-1} \quad \omega_n = 15545\text{ cm}^{-1} \quad \tau_n = 15\text{ fs}$$

$$\omega_0 = 380\text{ cm}^{-1} \quad d = 0.8 \quad \gamma_{el} = 0.9 \quad \gamma_{vib} = 0.1 \quad \omega_c = 700\text{ cm}^{-1}$$

### Results:

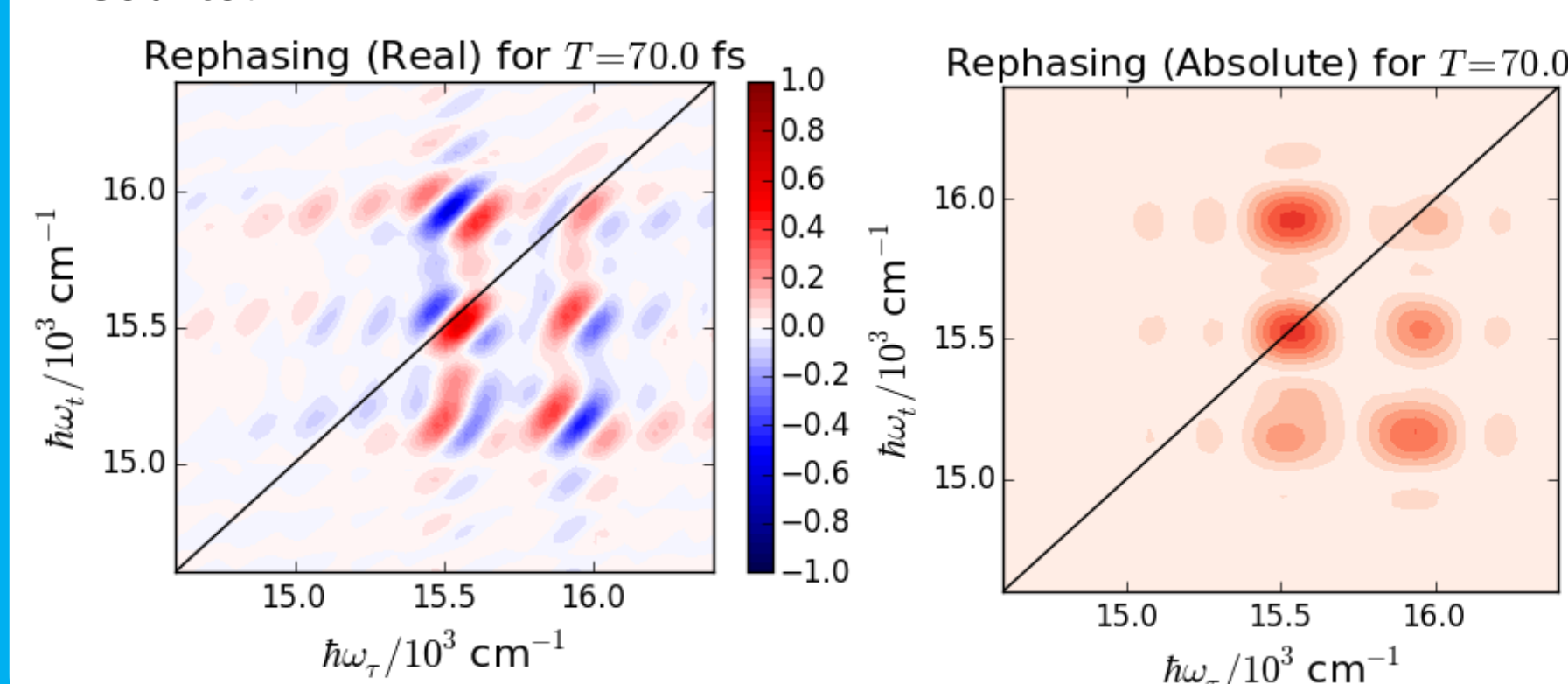


Figure 5: Real (left) and absolute (right) component of calculated rephasing 2D spectrum for a population time of  $T = 70$  fs.

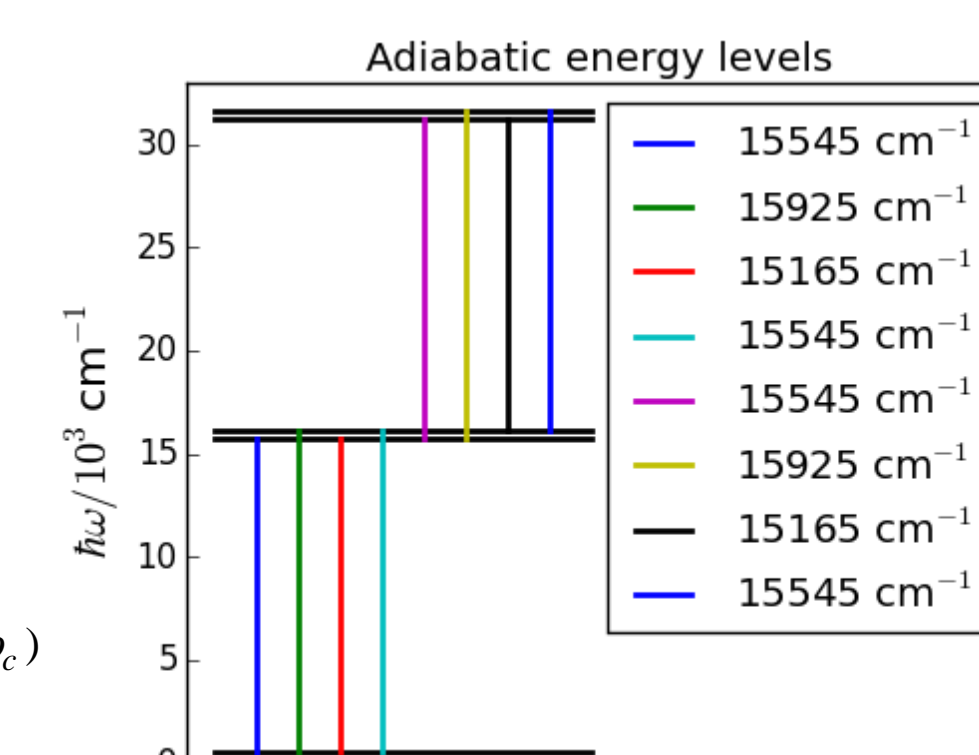


Figure 3: Calculated energy levels with transition frequencies labelled.

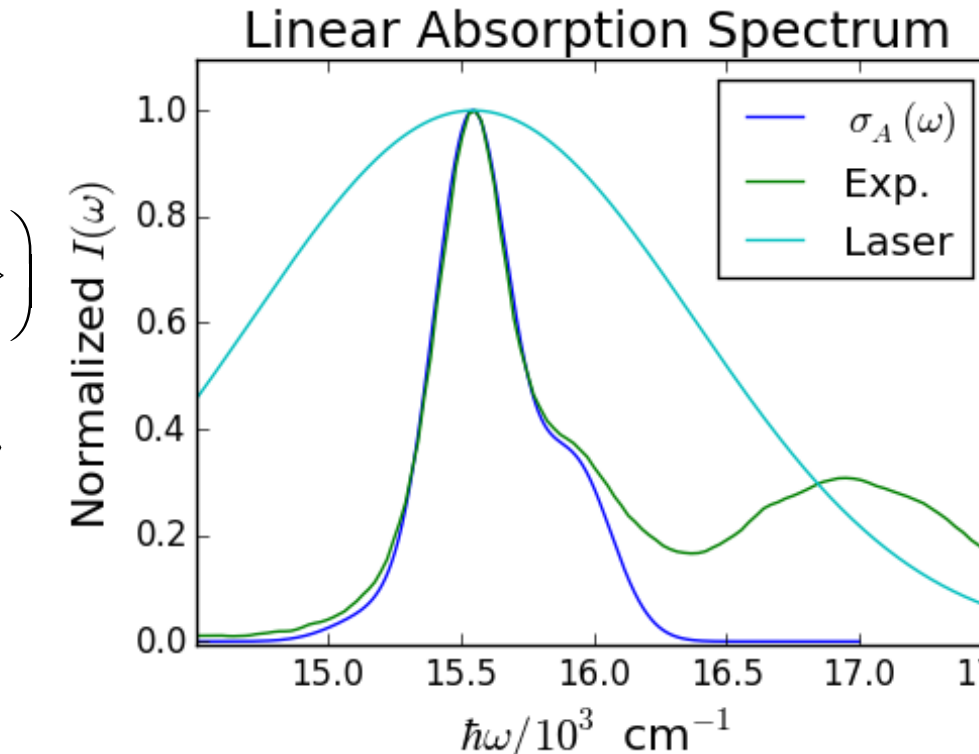


Figure 4: Calculated,  $\sigma_A(\omega)$ , and experimental, Exp., absorption spectra, with laser spectrum.

The resulting rephasing spectra show the expected 'chair' formation of peaks, but no inhomogeneous broadening due to the use of Markovian dynamics.

## Multimode Brownian Oscillator Model

### Theory:

The system is defined by the electronic states only, all nuclear motions are incorporated into the spectral density,  $C(\omega)$ . The intramolecular vibration is described by an underdamped mode,  $C_u(\omega)$ ; intermolecular vibrations for solvent interactions by overdamped modes,  $C_o(\omega)$ .<sup>3</sup>

$$C_u(\omega) = \frac{2\lambda\omega\omega_0^2\gamma}{(\omega_0^2 - \omega^2)^2 + \gamma^2\omega^2} \quad C_o(\omega) = 2\lambda \frac{\omega\Lambda}{\omega^2 + \Lambda^2}$$

Each excited state has a separate spectral density, which are assumed equal so all lineshape functions are equivalent.<sup>4</sup>

The addition of pathways involving the second excited state introduces ESA into the rephasing,  $R_R$ , and non-rephasing,  $R_{NR}$ , response functions.

### Results:

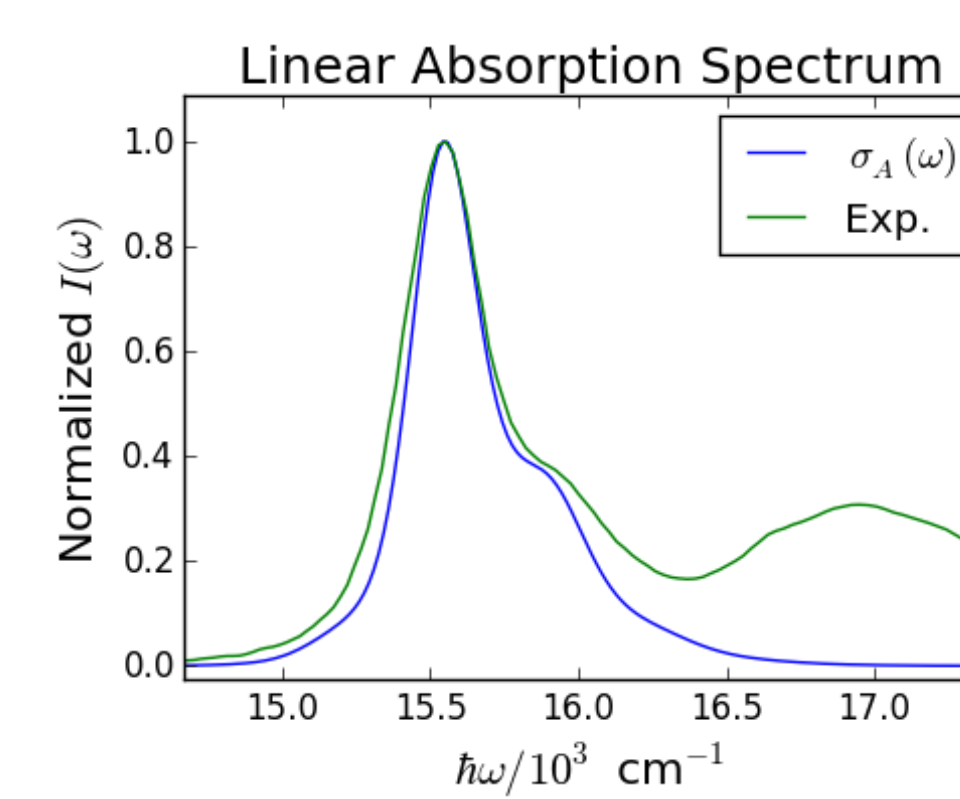


Figure 7: Calculated,  $\sigma_A(\omega)$ , and experimental, Exp., absorption spectra.

Parameters (at 300 K)		
$\omega_{eg}^0 = \omega_{fe}^0 = 15510\text{ cm}^{-1}$	$\omega_0 = 380\text{ cm}^{-1}$	$d = 0.8$
$\gamma\text{ (cm}^{-1}\text{)}$	$\lambda\text{ (cm}^{-1}\text{)}$	$\Lambda\text{ (cm}^{-1}\text{)}$
$C_{u1}$	100	122
$C_{o1}$	-	19
$C_{o2}$	-	21
		83.3

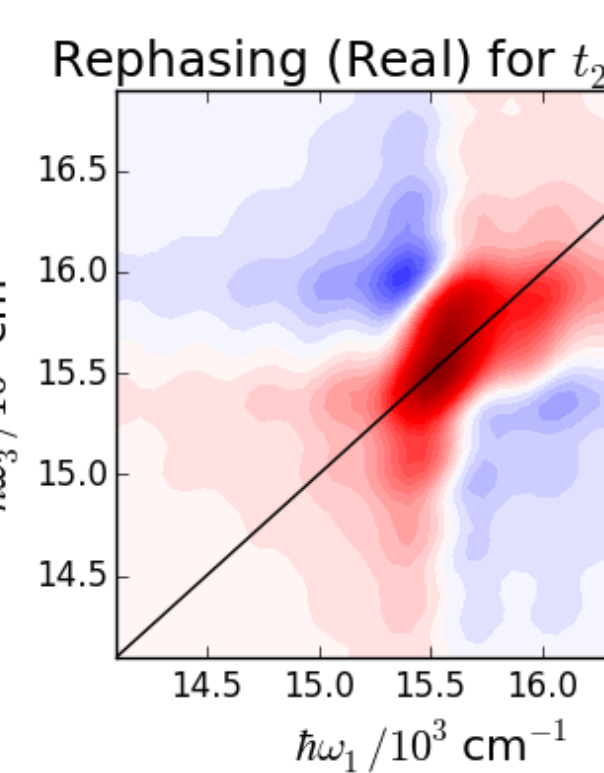


Figure 8: Real component of calculated rephasing (left) and non-rephasing (right) 2D spectra for a population time of  $t_2 = 70$  fs.

## Experimental 2D Spectra

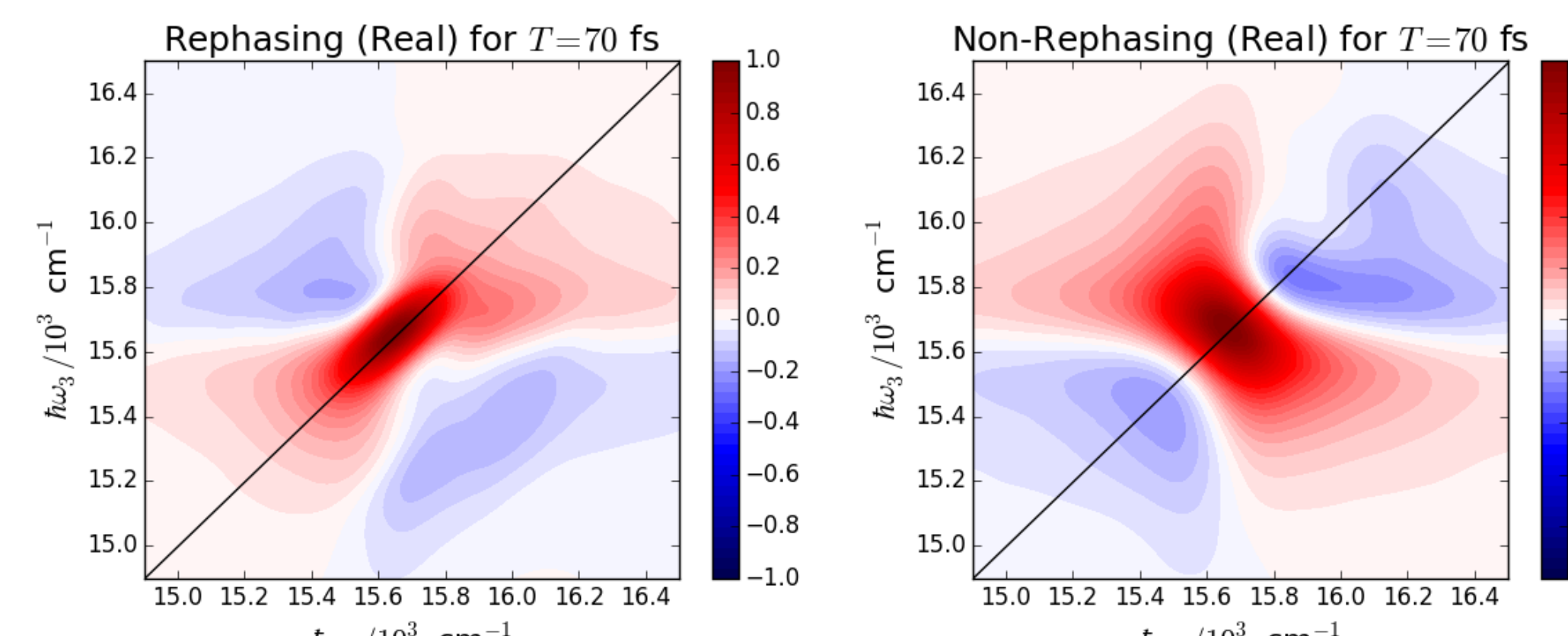


Figure 9: Real component of measured rephasing (left) and non-rephasing (right) 2D spectra for a population time of  $T = 70$  fs.<sup>2</sup>

## Summary and Objectives

At this stage, both the MBO and EOM-PMA models are producing recognisable 2D spectra for the *Q* band of the zinc-porphyrin chromophore. Methods have also been identified to expand the system definition to include an additional excited state, representing the *N* band.

- Improve line shape of EOM-PMA spectra by implementing non-Markovian dynamics.
- Improve representation of the breadth of the *N* band, regarding the use of unequal spectral densities for MBO and efficient incorporation of a vast number of new energy levels in EOM-PMA.
- Explore the influence of variable laser spectra in EOM-PMA vs. impulsive MBO.
- Extend the systems to include additional vibrational modes and/or dimers and larger aggregate structures.

## Acknowledgements

We would like to thank the University of East Anglia for funding and the Research and Specialist Computing Support Team at UEA for their continued assistance with use of the High-Performance Computing cluster.

## References

- F.V.A. Camargo, H.L. Anderson, S.R. Meech, and I.A. Heisler, *J. Phys. Chem. A* **119**, 95 (2015).
- F. V. de A. Camargo, L. Grimmelmann, H.L. Anderson, S.R. Meech, and I.A. Heisler, *Phys. Rev. Lett.* **118**, 33001 (2017).
- S. Mukamel, *Principles of Nonlinear Optical Spectroscopy* (Oxford University press, 1995).
- T. Brixner, T. Mančal, I. V. Stiopkin, and G.R. Fleming, *J. Chem. Phys.* **121**, 4221 (2004).
- M.F. Gelin, D. Egorova, and W. Domcke, *Acc. Chem. Res.* **42**, 1290 (2009).